Characterisation of cortical activity in response to deep brain stimulation of ventral lateral nucleus: Modelling and Experiment

Mohit H. Adhikari[a], Joost H. Heeroma[b], Mario di Bernardo[a], Bernd Krauskopf[a], Mark P. Richardson[c], Matthew C. Walker[b], John R. Terry[a]

[a]*Department of Engineering Mathematics, University of Bristol, Bristol, BS8 1TR, United Kingdom*
[b]*Department of Clinical and Experimental Epilepsy, Institute of Neurology, University College London, London, WC1N 3BG, United Kingdom*
[c]*Institute of Psychiatry, King's College London, SE5 8AF, United Kingdom*

Abstract

Motivated by its success as a therapeutic treatment in other neurological disorders, most notably Parkinson's desease, Deep Brain Stimulation (DBS) is currently being trialled in a number of patients with drug unresponsive epilepsies. However, the mechanisms by which DBS interferes with neuronal activity linked to the disorder are not well understood. Furthermore, there is a need to identify optimized values of parameters (for example in amplitude/frequency space) of the stimulation protocol with which one aims to achieve the desired outcome.

In this paper we characterize the system response to stimulation, to gain an understanding of the role different brain regions play in generating the output observed in EEG. We perform a number of experiments in healthy rats, where the ventral-lateral thalamic nucleus is stimulated using a train of square-waves with different frequency and amplitudes. The response to stimulation in the motor cortex is recorded and the drive-response relationship over frequency/amplitude space is considered. Subsequently, we compare the experimental data with simulations of a mean-field model, finding good agreement between the output of the model and the experimental data - both in the time and frequency domains - when considering a transition to sustained oscillatory activity in the cortex as the frequency of stimulation is increased.

Overall, our study characterises the drive-response relationship of DBS in healthy animals. In this way, it constitutes a first step towards the goals of developing a closed-loop feedback control protocol for suppressing epileptic activity, by adaptively adjusting the stimulation protocol in response to EEG activity.

---

1. Introduction

Epilepsy is a serious neurological disorder with a lifetime incidence of approximately 1% worldwide. Almost one third of patients have a poor or absent response to most standard anti-epilepsy medications. In a minority of these cases, resective surgery can be a highly successful treatment, provided the epileptogenic zone (the brain region responsible for genesis of seizure activity) can be identified. Unfortunately, in the majority of cases, the epileptogenic zone is too dispersed, overlies regions of eloquent cortex, or simply can not be determined using standard localization techniques, hence surgery is not an option. As a result there is a need for novel treatment strategies and recently electrical stimulation of deep brain regions such as cerebellum, caudate nucleus and thalamus has emerged as a possible treatment option [30, 35]. The use of DBS is motivated primarily by its success as a therapeutic treatment in other neurological disorders, most notably Parkinson's disease [2, 22, 37].

Although focal epilepsy originates in cerebral cortex, propagation and clinical expression of seizures requires cortico-subcortical circuits [28]; therefore hypothetically, disruption of nodes in these circuits could prevent epileptic seizures from evolving. Several techniques have been developed, with encouraging results, including stimulation of the presumed seizure onset zone in the medial temporal lobe [3], stimulation of thalamic anterior nucleus [1, 13, 15, 17], subthalamic nucleus [15, 36], cerebellar cortex [4], caudate nucleus [30], post hypothalamus and zona incerta [9]. Stimulation of thalamic centromedian nucleus (CM) is the most widely-reported technique [1, 8, 31, 32, 33, 34, 35]. However, the evidence-base and rationale for thalamic DBS in epilepsy is limited. In particular, as noted by others [7, 12, 29], the multiplicity of anatomical targets coupled with many variable stimulation parameters create obstacles in generalising from multiple small experimental and clinical studies. Hence, the motivation for this paper is to

characterise the underlying mechanisms linking the stimulation input in the ventral-lateral nucleus of the thalamus and the system output, recorded via EEG from an electrode placed in the motor cortex. Our ultimate objective is to develop effective DBS protocols for suppression of epileptic seizures by using measured brain activity from EEG, ECoG or implanted depth electrodes as inputs into adaptive control algorithms that, in turn, determine the type of stimulus to one or more brain regions.

In order to characterise the system response under 'normal' conditions, we perform an experiment in healthy rats whereby the ventral-lateral thalamic nucleus is stimulated using periodic square wave pulses over a range of frequencies and amplitudes. We measure cortical response to stimulation using EEG from an electrode placed in the motor cortex. In this paper, we present initial results from two different experiments. The data from the first experiment shows that for low stimulation frequencies, the cortical response to a stimulation pulse is in the form of a spike followed by a return to the baseline activity. However, as the stimulation frequency is increased, this pattern of response makes a transition to a sustained oscillatory activity. In the second experiment, performed on a different animal at reduced stimulation intensity, this transition to sustained oscillatory activity is not observed.

In a desire to understand these significantly different responses to a similar stimulation protocol, we compare the experimental data with the results of simulations of a mean-field model that includes the predominate connections believed to be involved between ventral-lateral and reticular nuclei in the thalamus and motor regions in the cortex. Interestingly, these connections correspond to those in a previously studied mean-field model [19, 24]. Using parameter estimates considered by Robinson and co-workers [24, 25] as corresponding to 'healthy' activity, places the system in a steady-state region close to a transition to oscillatory behaviour. Under these conditions, we find that the results of the simulations match well with the data in the frequency domain. Further, it is of particular interest that there is also a good agreement between the experimental data and model simulations in the time domain. In particular, we show that by choosing model parameters appropriately, we find the following scenario. If the inhibition within the thalamus occurs at two time scales sufficiently different from each other, then the overall inhibitory effect is reduced and, hence, the excitation from

an external electrical stimulation can be sustained. We offer this as a plausible explanation for a sustained oscillatory response to periodic stimulations observed in the first experiment.

The underlying idea behind the results presented here is that a validated model will make it possible to develop and evaluate control strategies for suppression of epileptiform activity before testing them in experiments. As a final part of this paper, we present two simple examples of how control strategies may be developed for models of the type considered here.

2. Methods

In this section we provide details of the experimental and mathematical models, and of the computational tools we use to analyse the data.

2.1. Experimental Description

Young adult male Sprague-Dawley rats (∼300g/9 weeks) were anaesthetized with isoflurane and electrodes (Bilaney consultants, UK) were stereotactically inserted at the following coordinates: Bipolar stimulating electrodes (from Bregma posterior 2.12mm, lateral 2.5mm, depth 5.5 and 6.0mm), Monopolar recording electrode (from Bregma posterior 2.12mm, lateral 2.5mm, depth 1.5mm) [23]. This placed the stimulus electrodes in the ventro-lateral nucleus of the thalamus and the recording electrode in the motor cortex. A silver wire was placed subcutaneously to act as earth and recording reference. During placement tests, pulses were used to verify and optimize activation of the thalamo-cortical system. Electrodes were clustered in a pedestal (Bilaney consultants, UK) and fixed with dental cement and three skull screws.

The thalamic relay neurons in the ventral lateral nucleus make monosynaptic excitatory projections to principal cells in the motor cortex and interneurons in the thalamic reticular nucleus. The cortical principal cells project back to the thalamic relay and reticular neurons, completing the excitatory loop. The reticular neurons primarily project back to their corresponding relay neurons, thus producing feed-back and feed-forward inhibition. Stimulation of the ventral lateral nucleus consisted of 50 μs square pulses at a fixed intensity given in terms of the current passing through the stimulation electrodes. The

EEG data was recorded at a sampling frequency of 256 Hz, filtered at 100 Hz.

The experimental data presented in this paper comes from two different stimulation protocols. In each case, EEG data was collected over a period of two hours with stimulation delivered as follows.

2.1.1. Periodic/Monophasic
The frequency of stimulation varied from 0.5 Hz to 7.5 Hz, in steps of 0.5 Hz, at an input current of 2 mA during each stimulation. Subsequently stimulation was applied with frequencies 7.5 Hz, 8 Hz, 10 Hz, 15 Hz, 20 Hz and 25 Hz with an input current of 1.5 mA and finally at 30 Hz with an input current of 1 mA. Each stimulation lasted for 1 minute. The time intervals between successive stimulations ranged between 1 and 8 minutes. This was to allow for dissipation of acute changes in neuronal excitability that may have been induced by the stimulation.

2.1.2. Periodic/Biphasic
The frequency of stimulation varied from 1 Hz to 10 Hz and back to 1 Hz, in steps of 1 Hz, at an input current of 0.15 mA (baseline to peak) during each stimulation. Each stimulation lasted for 1 minute followed by 3 minutes of silence. Based upon the previous protocol, this interval of time was deemed appropriate to avoid any acute changes to neuronal excitability as a result of the stimulation.

2.2. Model Description:
The mathematical model we consider is motivated by the anatomical connectivity between the ventral lateral nucleus, the reticular nucleus and the motor cortex described in the previous section. The top panel of Figure 1 sketches the generic corticothalamic circuit with the appropriate excitatory and inhibitory connections.

The model we consider belongs to a class of lumped or mean-field, neural-mass models, developed from a number of studies [10, 14, 18, 21], specific examples of which have been used to describe cortical activity recorded through EEG [16, 26, 27]. This class of models considers the averaged response to an averaged input of a population of neurons in a specific region (such as the ventral lateral nucleus of thalamus) as a single entity, where the equations

used to model the response are based upon the experimental work of Freeman [10] (neural masses). Essentially the dynamical variables of each neural mass represent the local mean value of a physiological quantity at a position in the mass, averaged over a small patch of neurons.

The excitatory and inhibitory connections made between ventral lateral and reticular nuclei in the thalamus and the motor cortex are identical to those considered in our previous study of a cortico-thalamic model [19], consisting of excitatory pyramidal cells in the cortex and populations of excitatory thalamo-cortical and inhibitory reticular cells in the thalamus. Consequently it is this model that we consider in the present study. Each of the neural masses is represented by three variables: the average membrane potential ($V_a(\mathbf{r},t)$), the average firing rate ($\zeta_a(\mathbf{r},t)$) and the axonal field ($\phi_a(\mathbf{r},t)$); the subscript a is used to refer to each of the different masses. The average rate at which action potentials are fired by a neural mass is a sigmoidal function of the average membrane potential. The firing rate influences the propagation of action potential-fields ϕ_a via axons of the neural mass. The variation of the average membrane potential of a neural mass is governed by these incoming fields from the neural masses with which it is connected through synapses.

Under several approximations described in [19], the equations modelling the three fundamental processes discussed above can be reduced to a set of 8 delay differential equations. We include a term, ($A\phi_{ext}$), to represent the external electrical stimulation, which gives the set of equations:

$$\begin{aligned}
\frac{d}{dt}\phi_{Mo}(t) &= y(t) && (1)\\
\frac{d}{dt}y(t) &= \gamma_{Mo}^2[-\phi_{Mo}(t)+\zeta(V_{Mo}(t))]-2\gamma_{Mo}y(t) && (2)\\
\frac{d}{dt}V_{Mo}(t) &= z(t) && (3)\\
\frac{d}{dt}z(t) &= \alpha\beta[-V_{Mo}(t)+\nu_{MoMo}\phi_{Mo}(t)+\nu_{MoI}\zeta(V_{Mo}(t))+\nu_{MoVl}\zeta(V_{Vl}(t))]\\
&\quad -(\alpha+\beta)z(t) && (4)\\
\frac{d}{dt}V_{Vl}(t) &= w(t) && (5)\\
\frac{d}{dt}w(t) &= \alpha\beta[-V_{Vl}(t)+\nu_{Vln}\phi_n+\nu_{VlMo}\phi_{Mo}(t)+A\phi_{ext}(t)]
\end{aligned}$$

$$+\alpha\beta[\nu^{A}_{VlRe}\zeta(V_{Re}(t)) + \nu^{B}_{VlRe}\zeta(V_{Re}(t-\tau))] - (\alpha+\beta)w(t) \quad (6)$$

$$\frac{d}{dt}V_{Re}(t) = v(t) \quad (7)$$

$$\frac{d}{dt}v(t) = \alpha\beta[-V_{Re}(t) + \nu_{ReMo}\phi_{Mo}(t) + \nu_{ReVl}\zeta(V_{Vl}(t))] - (\alpha+\beta)v(t) \quad (8)$$

Here ϕ_{Mo} is the average electrical activity of cortical cells that represents the EEG, V_{Mo}, V_{Vl} and V_{Re} are the average membrane potentials of the cortical cells and the ventral lateral and of the reticular nuclei of the thalamus, respectively. The average firing rate of a neural mass is represented by ζ, which is a sigmoidal function of the corresponding potential. Various ν_{ab} represent the average interaction (synaptic) strengths between different nuclei.

The term $A\phi_{ext}(t)$ (representing the stimulation input) is added to the term $\frac{dw}{dt}$ in equation (6) corresponding to a stimulation applied to the ventral lateral nucleus of the thalamus. Since we are considering healthy activity, the parameters of the model are chosen so that in the absence of stimulation the baseline activity corresponds to a steady-state [26]. Our previous analysis of this system [19] identified specific parameters, corresponding to cortico-thalamic excitability (ν_{VlMo}) and the effect of GABA_B activation (τ) that gave rise to transitions (termed bifurcations in the mathematical literature) between 'healthy' (pre-seizure activity) and seizure states. Understanding these transitions plays an important role in understanding the system response to stimulation.

Further, the functional form for ϕ_{ext} is chosen such that it represents square wave pulses of exactly 50 μs duration. The frequency of this stimulation is chosen to be in the same range as the two stimulation protocols used in the experiments for corresponding values of the amplitude A. Gaussian white noise is added to equation (6) through the subthalamic input term $\nu_{Vln}\phi_n$.

The delayed nature of system (1)–(8) stems from the fact that, as per Marten et al. [19], we model delayed inhibition of the activity in the specific relay nucleus by the reticular nucleus [6]. More specifically, the term $\nu^{B}_{VlRe}\zeta(V_{Re}(t-\tau))$ in (6) reflects the slower timescale of activation of $GABA_B$ receptors in the relay nucleus in comparison with that of $GABA_A$ receptors. The time delay τ is hence an additional parameter of the system and it was shown to influence where one finds the boundary of onset of oscillatory behaviour

[19]. Mathematically, the fact that we are dealing with a delay differential equation means that the evolution of the system is determined not simply by the state at a single point in time t_0, but rather by given function segments of the eight variable over the entire time history segment $[t_0 - \tau, t_0]$; see [11] for details. The simulations of (1)–(8) presented here were performed by numerical integration with a fourth-order Adams-Bashforth method, where we started from a constant initial function defined over an interval of length τ.

3. Results

In this section we consider results from both experimental protocols, as well as simulations and analysis of the model (1)–(8). Analysis of the model enables us to characterise salient features of the data. To this end, we compare samples of EEG measurements with time-series from the model, and observe good agreement between experiment and model. Furthermore, we present comparisons in the frequency domain, where we use a waterfall diagram representation of sets of frequency spectra of the system response as a function of the input frequency. In this way, we are able to determine for different driving protocols the relationship between input and output frequencies for measured data and for the model simulations, where we again observe good agreement. Analysis of the model enables us to characterise salient features of the data. Based on these comparisons, we provide possible explanations for the experimentally observed changes as the stimulation frequency is increased.

3.1. Experimental Observations

A number of separate experiments were performed using both protocols defined in the previous section. In Figure 2, we present samples from one such experiment under the first protocol. For low stimulation frequencies (< 3 Hz), the cortical response takes the form of a spike followed by a decay to 'baseline' (panel a)) activity (see Panels b) and c) of Figure 2). However, as the stimulation frequency is increased, the response is markedly different. In these cases (see Panels d), e) and f)), the cortical response is in the form of a sustained oscillation, whose frequency corresponds to that of the stimulation frequency. Most strikingly, in response to a 7 Hz stimulation (Panel f)) the cortical response has a near epileptiform appearance, despite there

being no physical manifestation of a seizure during this period of stimulation. Contrasting this scenario with samples presented from a different experiment under the second protocol in Figure 3, we observe no such sustained activity in cortical response for any given stimulation frequency.

It is interesting to speculate on possible mechanisms that might account for these marked differences in response. Could it simply be inter-animal differences in neural circuitry, precise placement of the electrodes or smaller amplitude of stimulation? Perhaps more significantly, during the quiet phase following the 3 Hz stimulation period of the first experiment, the animal underwent a spontaneous seizure (i.e. not as a direct consequence of the stimulation). This seizure, which had a characteristic frequency of cortical oscillation in the region of 2 Hz, was accompanied by significant motor responses (twitching). It was subsequent to this event that a cortical response in the form of a sustained oscillation was observed during each stimulation period. In the second experiment, where no seizure occurred, there was also no such sustained activity. Whilst it is only possible to speculate at this stage, this observation is in keeping with the work of Moraes and co-workers [5, 20] whose experimental studies suggest a connection between excitability of specific neural circuits and the occurrence of seizures. It would be quite plausible for excitability with specific circuits to persist post-seizure and the stimulation acts as a probe of this circuit, resulting in the observed sustained response. It is clearly desirable to perform further experiments to explore this interesting phenomena.

3.2. Comparison with model simulations

In order to investigate these experimental observations, we performed simulations of the mean-field model (1)–(8). From our previous studies of this system [19], suggested parameter values corresponding to healthy activity [25] place the system close to a transition to oscillatory activity (the Hopf bifurcation curve illustrated in panel b) of Figure 1). Consequently, when perturbed past this curve (for example via stimulation), the system may intrinsically oscillate with a characteristic frequency ω, the precise value of which is determined by an interplay between other model parameters. One parameter that influences this value significantly is the delay term τ, which models the different timescales of interaction between $GABA_A$ and $GABA_B$ receptors.

Significantly, the model is able to reproduce the transition in cortical response to stimulation from a decay to baseline to one of sustained oscillations, as is illustrated in Figure 4. Here we consider the scaled variable $\phi_{Mo}(t)$, corresponding to the excitatory cortical field potential, obtained by integrating the model equations with 50 μs square pulse stimulations at 2Hz and 7Hz, respectively. The parameter τ was chosen to be $0.03s$, giving an intrinsic system frequency close to 6Hz. This is then compared with the corresponding EEG traces from motor cortex during 2Hz and 7Hz stimulations (Panels a) and e) of Figure 2). Note the similarity in cortical response for different frequencies of stimulation, in addition to the increase in amplitude of response for higher frequency of stimulation.

Subsequently, we investigated whether the model could reproduce the findings of the experiment using the second protocol, where no transition to sustained activity occurred upon varying the stimulation frequency. We found that model simulations upon varying the parameter τ to values close to zero, whilst remaining in the 'healthy' regime to the left of the Hopf curve, were in good agreement with the data presented in Figure 3. In this case, there was only a spike and subsequent decay to baseline, for the entire range of frequencies used in the protocol, as illustrated in Figure 5.

We should comment at this stage that differences in experimental protocol, in particular the difference in stimulation amplitude (2mA as opposed to 0.15mA) might account for these differences. However, our model simulations suggest that underlying physiological mechanisms could also play an important role. In the case of the first experiment, to observe a transition to sustained activity upon increase of stimulation frequency placed model parameters (in particular the value of τ) in a region where increases in cortical excitability may actually give rise to seizure-like activity (spiking behaviour) (see panel a) Figure 4 of [19]). However, the values of τ needed to produce model simulations in keeping with the second experiment, placed the system in a region of parameter space where spiking behaviour could not be observed, no matter how significant an increase in cortical excitability. This finding is reminiscent of the experimental findings: in the first case the animal experienced a spontaneous seizure, whereas no seizures occurred during the experiment. We would expect the stimulation to have acute effects on system parameters, which may become chronic as a result of repeated seizures.

Another interpretation of the observed phenomena is that in the limit $\tau \to 0$, the maximum inhibition of the activity of the ventral lateral nucleus is greater than the corresponding amount in the case of a larger value of the delay. This is because the average membrane potential, and hence the average firing rate of the reticular nucleus, peaks at a specific instant of time. This, in turn, implies that the strength of inhibition at this instant of time will be greater in the case $\tau \to 0$ than otherwise. Thus, the electrical activity of neurons from the ventral lateral nucleus, and in turn that of the cortical cells, in response to stimulation, will return to baseline faster in the case $\tau \to 0$ than otherwise.

By keeping the distance to the Hopf curve constant, we can plot out in the delay-frequency space the transition to a sustained oscillatory response for a fixed amplitude of stimulation. This is presented in Figure 6.

3.3. Characterisation of drive-response frequency relationship

To explore further this relationship between the frequency of thalamic stimulation and that of the cortical response, we consider the power spectrum of EEG during stimulation, from the experimental recordings, as a function of the driving frequency. We compare these to the Fourier transforms of the equivalent output from simulations of the mean-field model (1)–(8), performed using the equivalent frequencies of stimulation as those in the experimental recordings. The respective spectra are presented in Figures 7 and 8 as three-dimensional plots of sets of spectra for the chosen driving frequencies; one also refers to this representation as waterfall diagrams. These figures confirm our initial observation from the raw EEG that the main response of the cortical activity appears at the stimulation frequencies as exhibited by the largest peaks in the spectrum along the lead diagonal.

More specifically, the top panel of Figure 7 shows the power spectrum of the EEG during stimulations periods under protocol one, as a function of the driving frequency (from 0.5 to 7.5 Hz). Although the EEG was recorded for sixty seconds, the Fourier transform was performed only over a forty second time window, because of the presence of large stimulation artefacts at the beginning of some of the stimulations. The main response of the cortical activity appears at the equivalent stimulation frequency as exhibited by the large peaks in the spectra along the lead diagonal of the waterfall

diagram. These are augmented by several harmonic responses, as demonstrated by peaks at multiples of the stimulation frequency to the right of the lead diagonal. There is also significant activity in the extremely low frequency region ($\sim$0.1 Hz). For low driving frequencies (less than 2.5 Hz), this response seems more significant than that in the region close to the stimulation frequency. This activity can be partially attributed to non-stationarity of the EEG (manifesting itself as a slow frequency related to the sampling frequency used to calculate the power spectrum), as well as the possibility of the animal sleeping during the experiment.

The bottom panel of Figure 7 plots the power spectrum of scaled output of the model (ϕ_{Mo}) as a function of the driving frequency (from 0.5Hz to 8Hz). In a similar manner to the experiment, the dominant response of the model also occurs at the stimulation frequencies. However, as we discussed in the previous section, the model parameters are set in the steady state region close to a Hopf bifurcation. If one crosses the Hopf bifurcation curve (in Figure 1, bottom panel) horizontally from left to right, the solution of the model will oscillate at the intrinsic frequency of the system ω. Hence we see an increase in the maximum power of the system as the stimulation frequency and the intrinsic frequency coincide (in this case at 6 Hz). An equivalent preference for a particular frequency is not apparent in the experimental data, where the maximum power remains fairly consistent across the range of frequencies considered.

In the top panel of Figure 8 we again present the power spectrum of EEG during stimulation, this time recorded under the second protocol, as a function of the driving frequency (from 1 to 10 Hz). The main response of the cortical activity again appears at the stimulation frequencies as exhibited by the peaks at the diagonal of the waterfall diagram. Under protocol two, biphasic stimulation and a smaller intensity (0.15 mA) were used, compared with 2 mA monophasic stimulation used under protocol one. Interestingly, the power in the main frequency band observed did not scale linearly with stimulation intensity. This increased response may be partially attributed to the biphasic nature of the stimulation. However, it is more likely due to inter-animal differences, where the excitability of specific neural circuits involved in the cortico-thalamic loop would be different. In terms of model parameters, these differences can be accounted for by the location in parameter space, relative to the Hopf curve. The bottom panel of Figure 8 presents

the response of the model under the same simulation protocol.

4. Discussion

In this paper we present preliminary findings from an experimental and modelling study designed to characterise the cortical response to deep brain stimulation of the ventral lateral thalamic nucleus. The experimental data was collected under two different stimulation protocols, where a range of stimulation frequencies and amplitudes were considered. These were compared to numerical simulations of a mean-field neural mass model, incorporating the regions believed to be involved in the experimental model.

The main response from the cortex appeared when periodic stimulations were used in the experiments. The results of the corresponding simulations in the model agreed with this observation. There was also a good agreement between the output of the model and the recorded EEG. In particular, a transition to sustained oscillatory activity in the cortex was observed as the frequency of stimulation was increased at a sufficiently high intensity. By adjusting the model parameters, we were able to demonstrate this transition in the model output and provide a possible explanation for its occurrence. Specifically, we showed that, for sufficiently high values of the time delay in the model (i.e. by considering a slower timescale of the inhibitory $GABA_B$ receptors in comparison with that of $GABA_A$ receptors) the inhibition of the activity of the ventral lateral nucleus is reduced, leading in effect to greater excitability in the system. If, instead, the timescales of $GABA_A$ and $GABA_B$ receptors are comparable, the inhibition is observed to be strongest and hence the excitation is not sustained for higher frequencies. This was observed in the second data set, which matched with the corresponding simulations in the model when the time delay was reduced to almost zero.

Thus, we conclude that the model presented here enables the characterisation of cortical response to electrical stimulation of a thalamic nucleus in healthy animals. The next step will be to consider the characterisation of cortical response in the case of an animal model of focal epilepsies. This will enable us to tune model parameters in order to characterise the response in both cases.

Ultimately we would like to use techniques from control theory to develop stimulation protocols to suppress seizure activity in diseased animals. The

idea is to use the stimulation electrode as a control input and devise feedback control protocols to suppress seizure activity. From this viewpoint, the design will be highly enhanced by the availability of a model, such as the one described in the paper. Indeed, having validated a model that characterises the cortical response to the electrical stimulation of a thalamic nucleus, any protocol can be designed, validated and tested *in silico* before any *in vivo* experiment is carried out.

Ongoing investigations appear to show that controlled stimulations can be effective in changing the model dynamics. As an example that supports this assertion, we present the results of simulations of the model with the inclusion in Equation (1)–(8) of two choices of linear feedback controllers of the form $\phi_{\text{ext}} = k\phi_{Mo}$ where k is a constant negative gain. With this type of controller, we are able to suppress oscillations. Specifically, we chose $\tau = 0.03$s and $\nu_{VlMo} = 1.78e-4$Vs, i.e., we placed the model in the region to the right of the Hopf curve drawn in the bottom panel of Figure 1, so that, in the absence of the controller, we find a stable oscillatory solution with a frequency of about 6 Hz. The two linear feedback controllers we used are an instantaneous and a delayed feedback laws of the form (a) $k\phi_{Mo}(t)$, and (b) $k\phi_{Mo}(t-\delta)$ where δ is a time delay chosen as part of the control design stage. As Figure 9 shows, the oscillatory solution decays to steady state when the controller is turned on in both cases. When the delay is chosen to be half the period of the oscillation of the uncontrolled system, the time of decay to steady state for the delayed controller (b) is shorter than that for the instantaneous controller (a). These preliminary results seem to confirm the effectiveness of the model presented and validated in this paper for both experimental validation and control system design. This work will be used to address the issue of detailed synthesis of novel feedback control protocols to suppress seizures.

5. Acknowledgments

The authors are grateful to Marcio Moraes for useful discussions concerning excitability and neural circuitry, as well as assistance in automating the stimulation protocols used in the experimental model. We thank Jamie Walker and Oscar Benjamin for extensive discussions concerning system behaviour and help with the computer simulations. Financial support via the Millstein

Fund of the Medical Research Council (G0701050) is gratefully acknowledged.

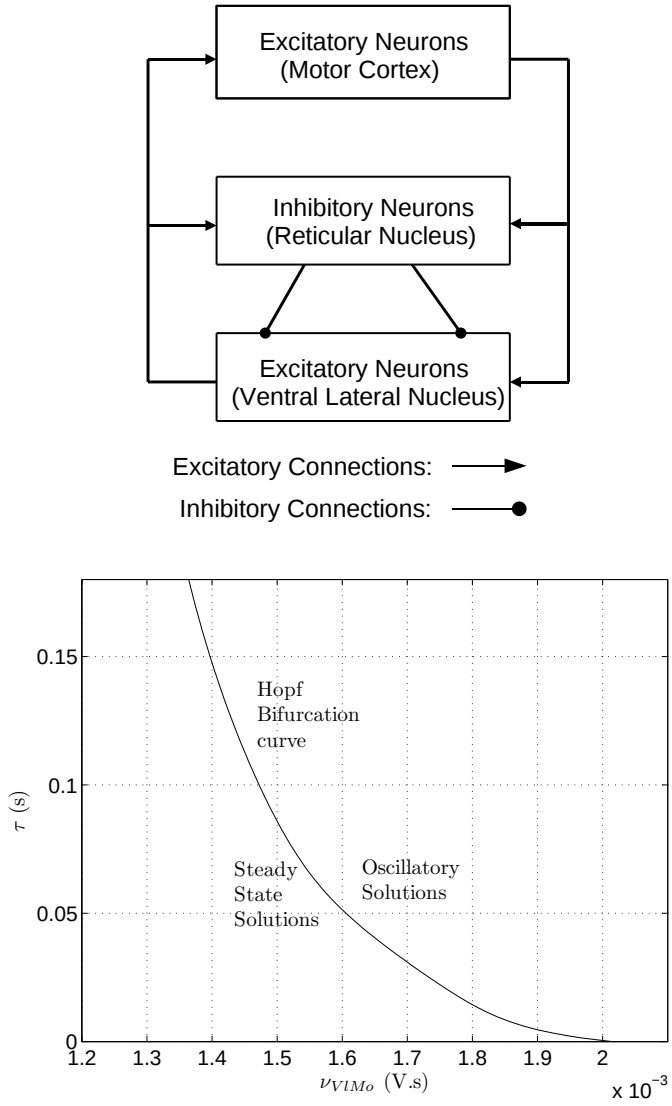

Figure 1: Top: Schematic of the corticothalamic model we consider, with inhibitory and excitatory connections based on known physiology. Interestingly, the connectivity between neural populations is equivalent to a previously considered model [19]. Bottom: The relevant parameter region of the model depicting a curve that marks the transition from the steady state solutions to the oscillatory solutions.

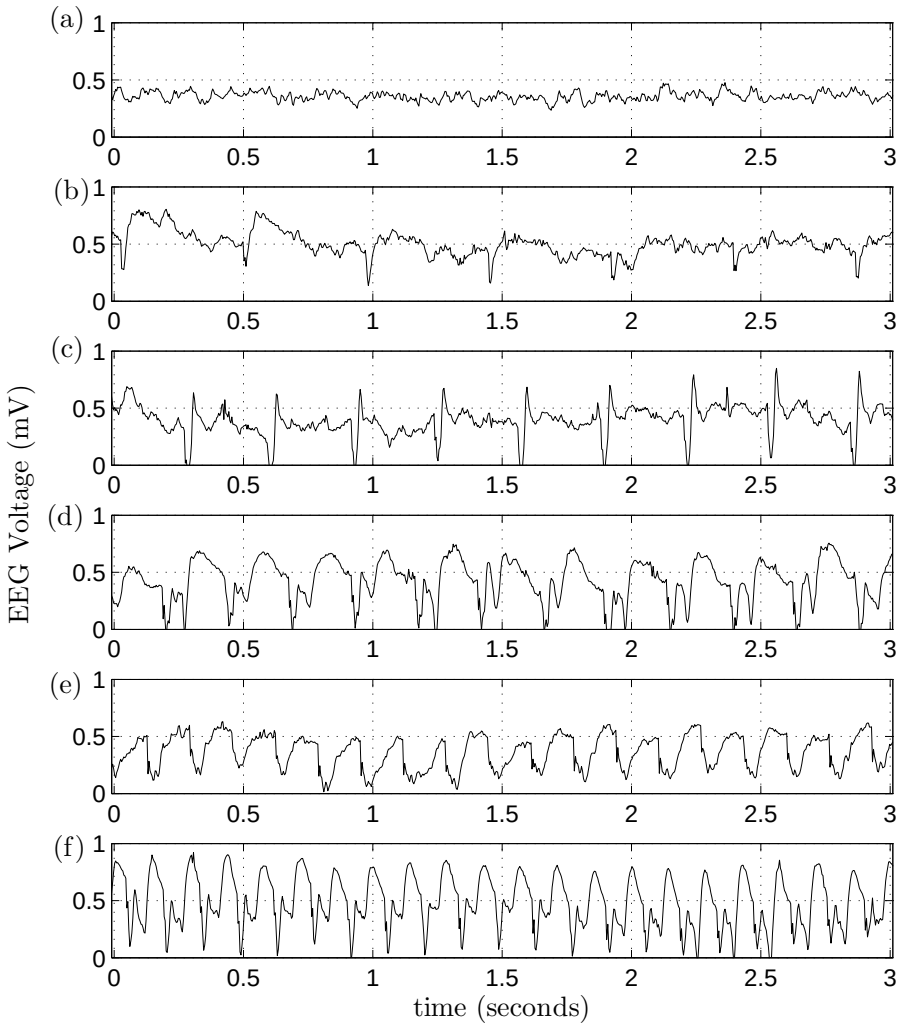

Figure 2: Presenting cortical activity recorded via EEG from an electrode placed in motor cortex. This activity was recorded during protocol 1 and we present baseline activity (a) and the response to stimulation at 2 Hz (b), 3 Hz (c), 4 Hz (d), 6 Hz (e) and 7 Hz (f). Whilst the cortical response appears to decay to baseline activity during stimulation at 2 and 3 Hz, a sustained oscillation is observed at 4, 6 and 7 Hz (panels d), e) and f)). At this stage this marked difference may only be speculated upon, but it could be as a consequence of a spontaneous seizure that occurred during the quiet phase following stimulation at 3 Hz.

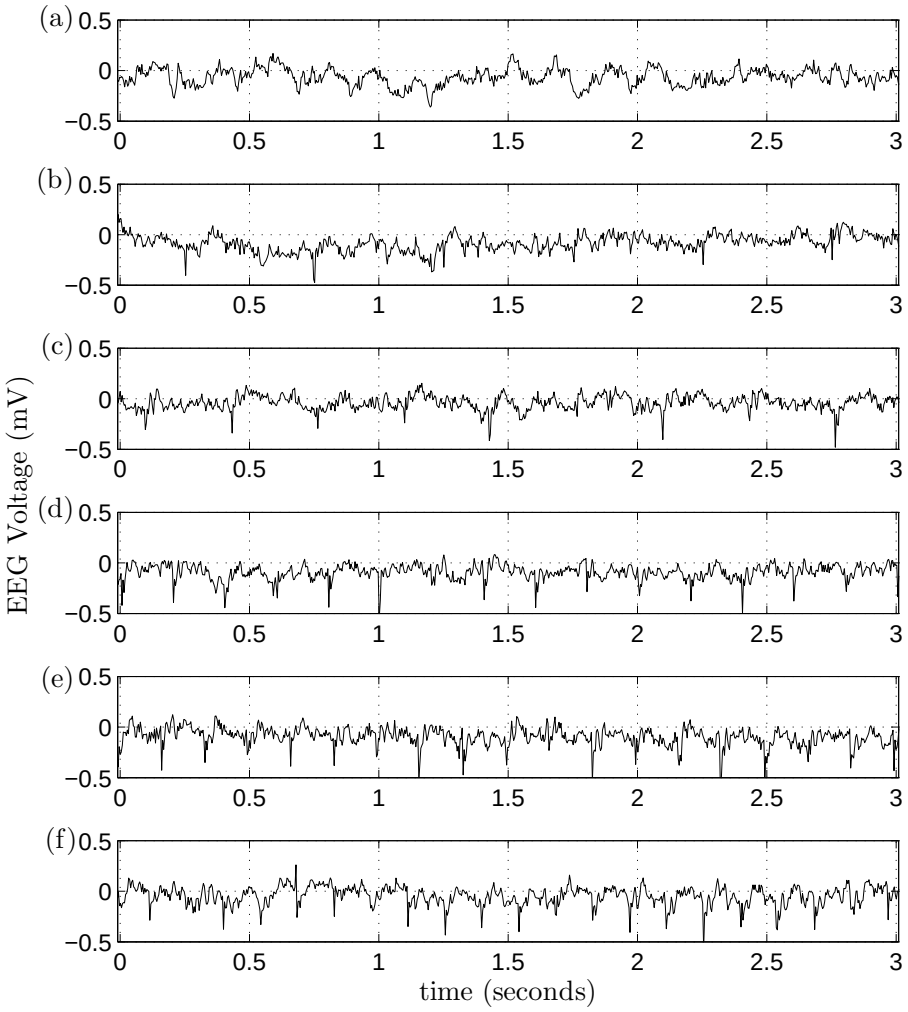

Figure 3: Presenting cortical activity recorded via EEG from an electrode placed in motor cortex. This activity was recorded during protocol 2 and we present baseline activity (a) and the response to stimulation at 2 Hz (b), 3 Hz (c), 5 Hz (d), 6 Hz (e) and 7 Hz (f). In contrast to the first experiment, we only observe a decay to baseline activity in response to stimulation at all considered frequencies.

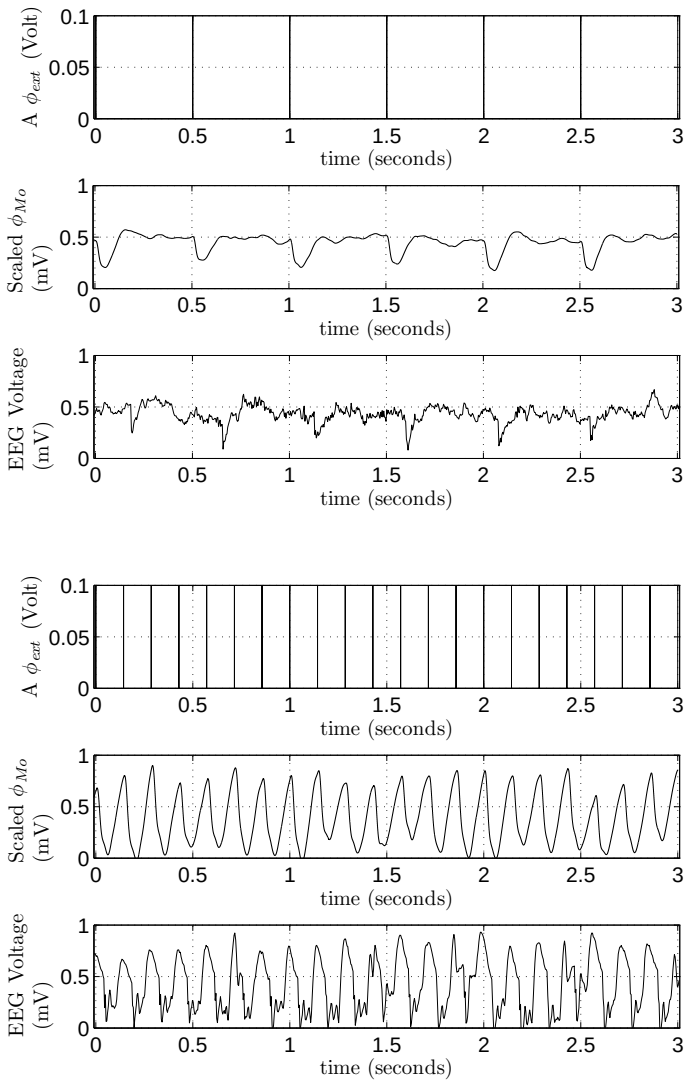

Figure 4: Comparison of the scaled output from the model in response to an input of square wave pulses of 50 μs duration at 2Hz (the top panel) and at 7 Hz (the bottom panel), with the corresponding data from experiment 1. The average amplitude of both the model output and the data at 7Hz is greater than at 2Hz, since the input intensity per pulse is kept the same. Here $\tau = 0.03s$ and $\nu_{VlMo} = 0.0016V.s$. The corresponding intrinsic frequency is 6 Hz.

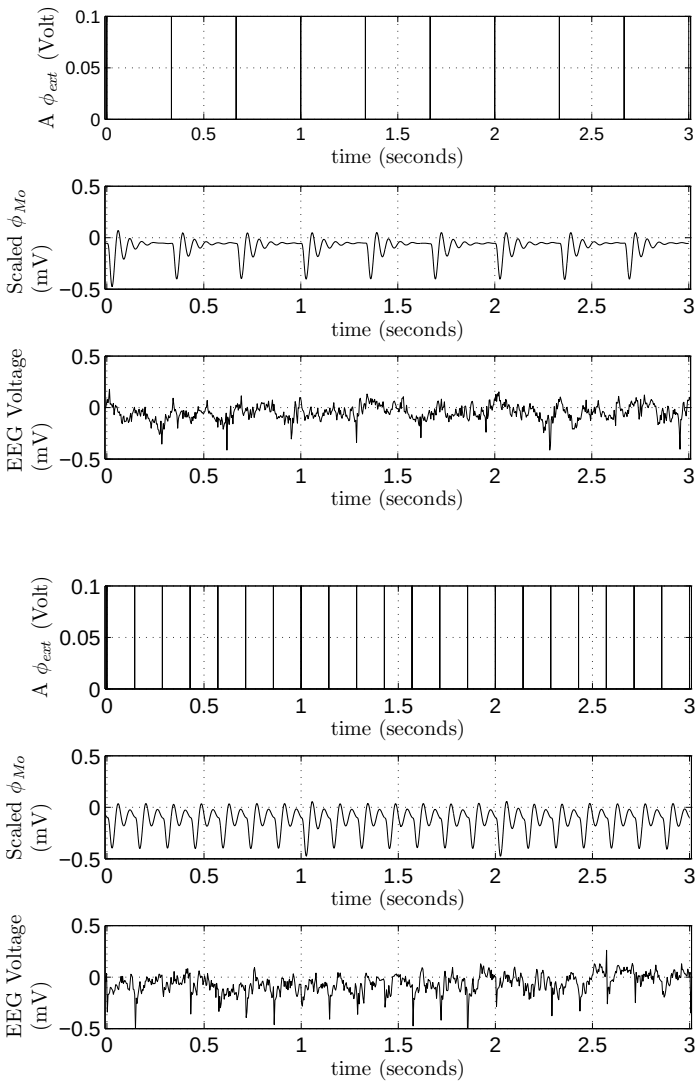

Figure 5: Comparison of the scaled output from the model in response to an input of square wave pulses of 50 μs duration at 3 Hz (the top panel) and at 7 Hz (the bottom panel), with the corresponding data from experiment 2. Both the model output as well as the EEG show a spike in response to each stimulation pulse followed by a return to the steady state activity and the oscillations do not seem to have been sustained even at 7 Hz. Here $\tau = 0.001s$ and $\nu_{VlMo} = 0.0018V.s$.

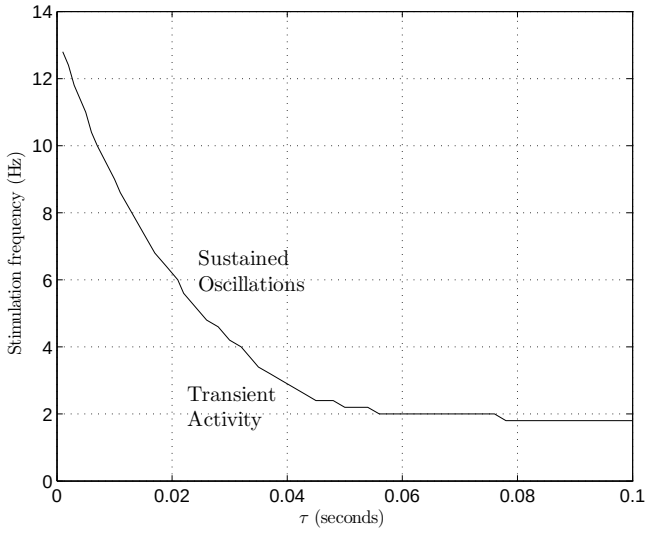

Figure 6: Consideration of the transition to sustained oscillations in the delay-frequency space, for a fixed horizontal distance ($1.0e-4$Vs) from the Hopf curve and for a fixed amplitude of stimulation (0.1 V). By sustained activity we mean an oscillatory response, for which no damped oscillations towards rest activity are observed. This difference in response may be thought of as the variation in stimulation response when comparing panels b) and c) to panels d), e) and f) of Figure 2.

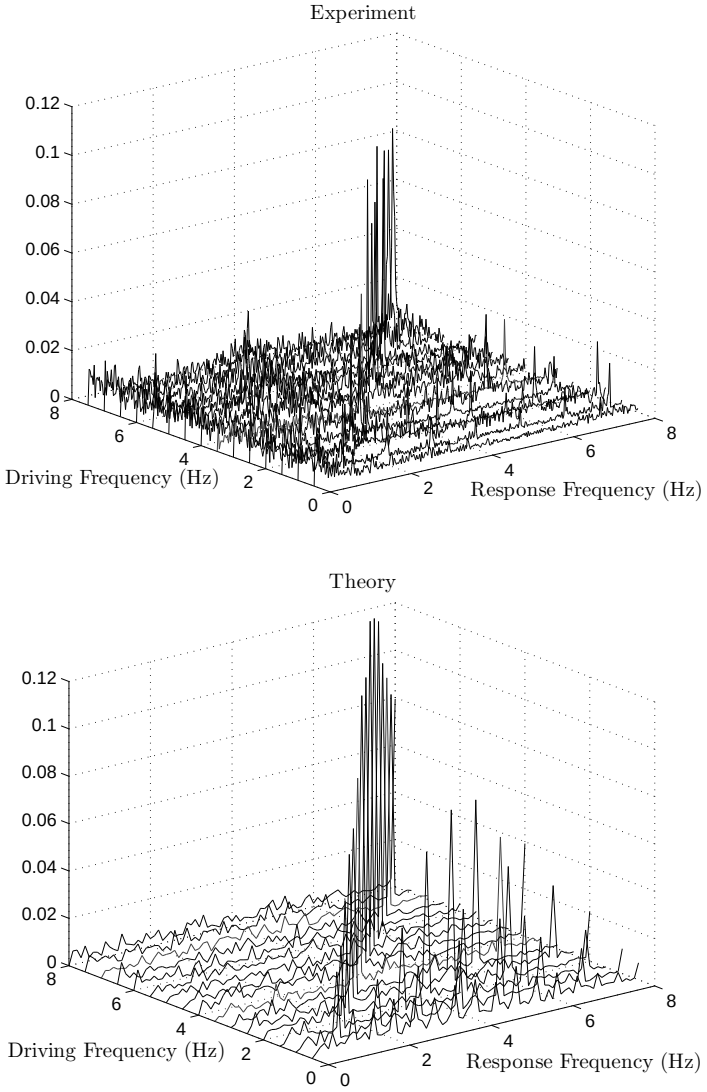

Figure 7: Top: Power spectrum of the data obtained using a 40 second window during stimulation, in experiment 1, plotted as a function of the driving frequency. The input current is constant at 2mA and the stimulation is monophasic. Bottom: Power spectrum of the model output plotted as a function of the driving frequency in response to monophasic stimulation. The stimulation amplitude is fixed at 0.1V and Gaussian white noise is added to the subthalamic input. The frequency response of both the model and the data appears at the stimulation frequency, however, there is no apparent preference for a frequency in the data as it is in the case of the model (at 6 Hz).

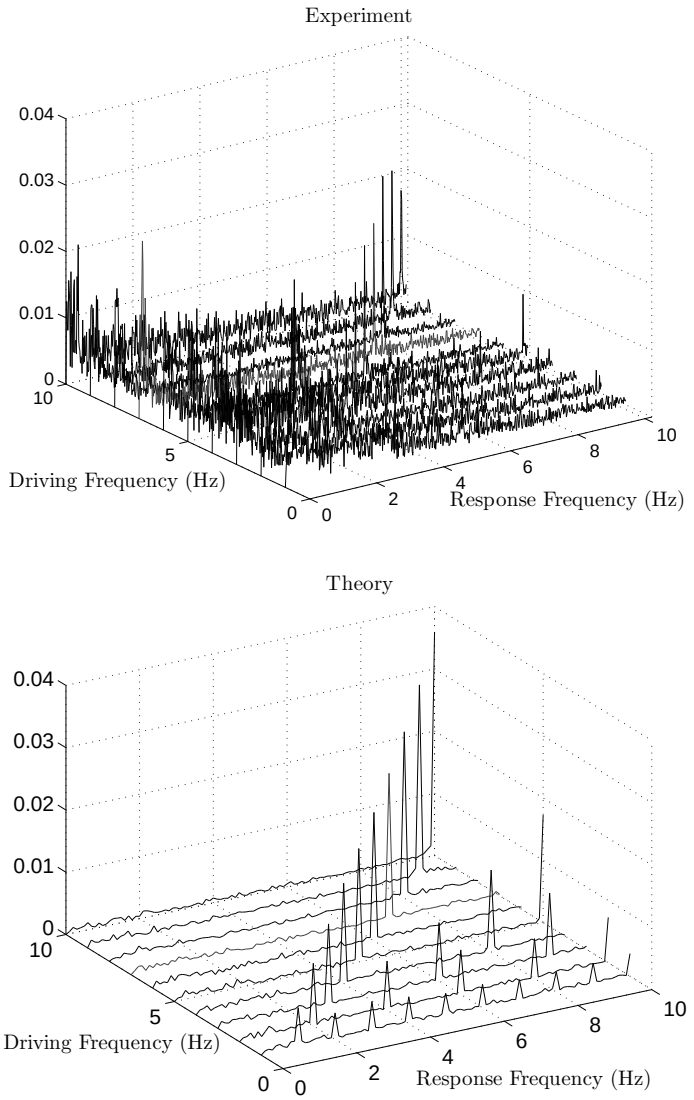

Figure 8: Top: Power spectrum of the data obtained using a 60 second window during stimulation, in experiment 2, plotted as a function of the driving frequency. The input current is constant at 0.15mA and the stimulation is biphasic. Bottom: Power spectrum of the model output plotted as a function of the driving frequency for $\tau = 0.001$s and $\nu_{se} = 0.0018$Vs. The stimulation amplitude is fixed at 0.1V and Gaussian white noise is added to the subthalamic input. Again, the frequency response of both the model and the data appears at the stimulation frequency, however, there is no obviously apparent preference for a frequency in the data. In the case of the model, the intrinsic frequency for this choice of parameters is close to 18 Hz.

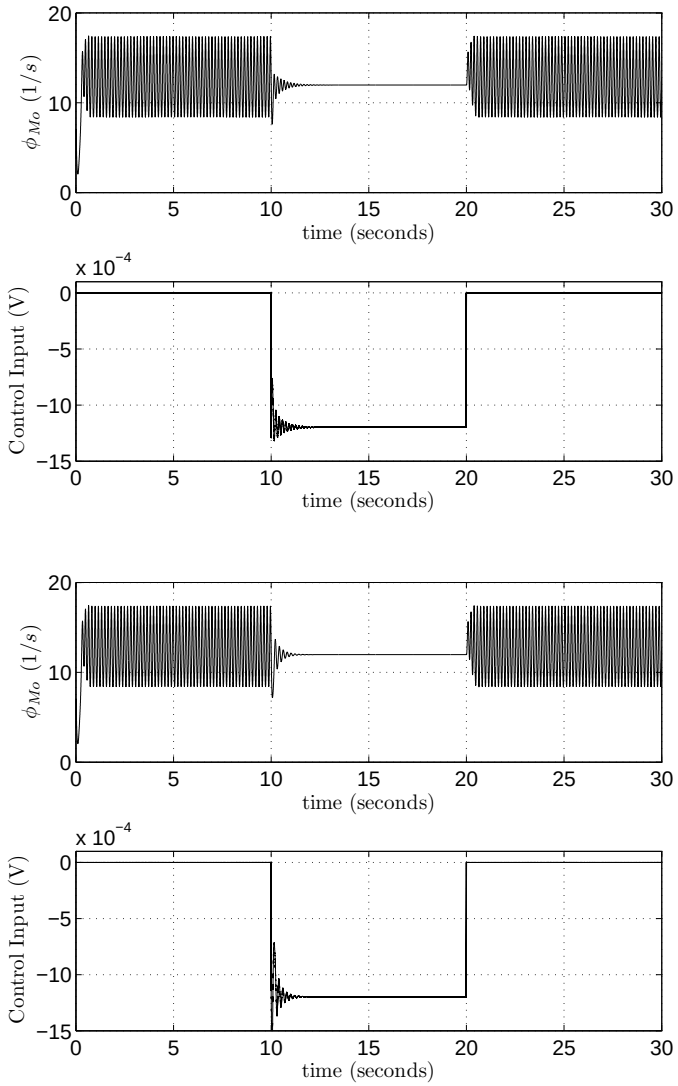

Figure 9: Model output in response to a linear feeback control (top two panels) and delayed linear feedback control (bottom two panels). The controller is turned on for a 10 seconds interval. Before the controller is turned on, the model output is oscillatory which decays to a steady state during the time the controller is on. The bottom two panels represent the situation when the output is delayed by half of the period of the oscillation of the uncontrolled system before it is fed back.

Quantity	Description	Value
θ	Threshold of membrane potential, before cells fire	0.015 V
σ	Standard deviation of firing rate	0.006 V
Q_{max}	Average maximum firing rate	250 s^{-1}
γ_e	Average ratio of pulse velocity to axon range	100 s^{-1}
α	Receptor offset time constant	50 s^{-1}
β	Receptor offset time constant	200 s^{-1}
τ	Time delay, due to slow $GABA_B$ response	varies
ν_{Vln}	subthalamic coupling	$20e-4$V s
ν_{MoMo}	Excitatory corticocortical coupling	$10e-4$V s
ν_{MoI}	Inhibitory corticocortical coupling	$-18e-4$V s
ν_{MoVl}	Specific thalamic to cortical coupling	$17e-4$V s
ν_{VlMo}	Cortical to specific thalamic coupling	varies
$\nu_{VlRe}^{A,B}$	$GABA_{A,B}$ thalamic relay to specific thalamic coupling	$-8e-4$V s
ν_{ReMo}	Cortical to thalamic relay nuclei coupling	$0.5e-4$V s
ν_{ReVl}	Specific thalamic to thalmic relay coupling	$5e-4$V s

Table 1: Parameter values for the model

References

[1] Andrade, D. M., Zumsteg, D., Hamani, C., Hodaie, M., Sarkissian, S., Lozano, A. M., Wennberg, R. A., 2006. Long-term follow-up of patients with thalamic deep brain stimulation for epilepsy. Neurology 66, 1571–1573.

[2] Assad, W., Eskandar, E., 2008. The movers and shakers of deep brain stimulation the movers and shakers of deep brain stimulation the movers and shakers of deep brain stimulation the movers and shakers of deep brain stimulation. Nature Medicine 14, 17–19.

[3] Boon, P., Vonck, K., de Herdt, V., van Dycke, A., Goethals, M., Goossens, L., van Zandijcke, M., de Smedt, T., Dewaele, I., Achten, R., Wadman, W., Dewaele, F., Caemaert, J., van Roost, D., 2007. Deep brain stimulation in patients with refractory temporal lobe epilepsy. Epilepsia 48 (8), 1551–1560.

[4] Cooper, I. S., Upton, A. R., Amin, I., 1982. Chronic cerebellar stimulation (ccs) and deep brain stimulation (dbs) in involuntary movement disorders. Appl. Neurophysiol. 45, 209–217.

[5] Cota, V. R., de Castro Medeiros, D., da Páscoa Vilela, M. R. S., Doretto, M. C., Moraes, M. F. D., 2009. Distinct patterns of electrical stimulation of the basolateral amygdala influence pentylenetetrazole seizure outcome. Epilepsy and Behavior 14 (1, Supplement 1), 26 – 31, international Symposium NEWroscience 2008 - Contemporary Neuroscience, Epilepsies and the Arts, International Symposium NEWroscience 2008.

[6] Destexhe, A., Sejnowski, T. J., 2001. Thalamocortical Assemblies. Oxford University Press.

[7] Ellis, T. L., Stevens, A., 2008. Deep brain stimulation for medically refractory epilepsy. Neurosurg. Focus 25, E11.

[8] Fisher, R. S., Uematsu, S., Krauss, G. L., Cysyk, B. J., McPherson, R., Lesser, R. P., Gordon, B., Schwerdt, P., Rie, M., 1992. Placebo-controlled pilot study of centromedian thalamic stimulation in treatment of intractable seizures. Epilepsia 33, 841–851.

[9] Franzini, A., Messina, G., Marras, C., Vilani, F., Cordella, R., Broggi, G., 2008. Deep brain stimulation of two unconventional targets in refractory non-resectable epilepsy. Stereotact. Funct. Neurosurg. 86, 373–381.

[10] Freeman, W., 2004. Mass Action In The Nervous System: Examination of The Neurophysiological Basis of Adaptive Behavior through The EEG. Academic Press, New York.

[11] Hale, J. K., Lunel, S. M. V., 1993. Introduction to Functional Differential Equations. Springer-Verlag, New York.

[12] Halpern, C. H., Samadani, U., Litt, B., Jaggi, J. L., Baltuch, G. H., 2008. Deep brain stimulation for epilepsy. Neurotherapeutics 5, 59–67.

[13] Hodaie, M., Wennberg, R. A., Dostrovsky, J. O., Lozano, A. M., 2002. Chronic anterior thalamus stimulation for intractable epilepsy. Epilepsia 43, 603–608.

[14] Jirsa, V. K., Haken, H., Jul 1996. Field theory of electromagnetic brain activity. Phys. Rev. Lett. 77 (5), 960–963.

[15] Lee, K. J., Jang, K. S., Shon, Y. M., 2006. Chronic deep brain stimulation of subthalamic ad anterior thalamic nuclei for controlling refractory partial epilepsy. Acta. Neurochir. Supp. 99, 87–91.

[16] Liley, D. T. J., Cadusch, P. J., Dafilis, M. P., 2002. A spatially continuous mean field theory of electrocortical activity. Network: Computation in Neural Systems 13 (1), 67–113.

[17] Lim, S. N., Lee, S. T., Tsai, Y. T., Chen, I. A., Tu, P. H., Chen, J. L., Chang, H. W., Su, Y. C., Wu, T., 2007. Electrical stimulation of the anterior thalamus for intractable epilepsy: A long-term follow-up study. Epilepsia 48, 342–347.

[18] Lopez da Silva, F. H., Hoeks, A., Smits, H., Zettberg, L. H., 1974. Model of brain rhythmic activity. the alpha-rhythm of the thalamus. Kybernetik 15, 27–37.

[19] Marten, F. B., Rodrigues, S., Benjamin, O. J., Richardson, M. P., Terry, J. R., 2008. Onset of poly-spike complexes in a mean-field model of human eeg and its application to absence epilepsy. Phil. Trans. Royal Soc.

[20] Moraes, M., Chavali, M., Mishra, P., Jobe, P., Garcia-Cairasco, N., 2005. A comprehensive electrographic and behavioral analysis of generalized tonic-clonic seizures of gepr-9s. Brain Research 1033 (1), 1 – 12.

[21] Nunez, P. L., 1974. The brain wave function: A model for the eeg. Mathematical Bioscience 21, 279–297.

[22] Olanow, C. W., 2004. The scientific basis for the current treatment of parkinson's disease. Annual Review of Medicine 55, 41–60.

[23] Paxinos, D. G., Watson, C., 1986. The Rat Brain in Stereotaxic Coordinates - The New Coronal Set. Academic Press, Sydney.

[24] Robinson, P. A., Rennie, C. J., Rowe, D. L., Apr 2002. Dynamics of large-scale brain activity in normal arousal states and epileptic seizures. Phys. Rev. E 65 (4), 041924.

[25] Robinson, P. A., Rennie, C. J., Rowe, D. L., O'Connor, S. C., 2004. Estimation of multiscale neurophysiologic parameters by electroencephalographic means. Human Brain Mapping 23, 53–72.

[26] Robinson, P. A., Rennie, C. J., Wright, J. J., Jul 1997. Propagation and stability of waves of electrical activity in the cerebral cortex. Phys. Rev. E 56 (1), 826–840.

[27] Robinson, P. A., Wright, J. J., Rennie, C. J., Apr 1998. Synchronous oscillations in the cerebral cortex. Phys. Rev. E 57 (4), 4578–4588.

[28] Spencer, S. S., 2002. Neural networks in human epilepsy: Evidence and implications for treatment. Epilepsia 43, 219–227.

[29] Theodore, W. H., Fisher, R., 2007. Brain stimulation for epilepsy. Acta. Neurochir. Supp. 97, 261–272.

[30] Theodore, W. H., Fisher, R. S., 2004. Brain stimulation for epilepsy. The Lancet Neurology 3 (2), 111–118.

[31] Velasco, F., Velasco, M., Jiminez, F., Velasco, A. L., Brito, F., Rise, M., Carilllo-Ruiz, J. D., 2000. Predictors in the treatment of difficult to control seizure by electrical stimulation of the centromedian thalamic nucleus. Neurosurgery 47, 295–304.

[32] Velasco, F., Velasco, M., Jiminez, F., Velasco, A. L., Marquez, I., 2001. Stimulation of the central median thalamic nucleus for epilepsy. Stereotact. Funct. Neurosurg. 77, 228–232.

[33] Velasco, F., Velasco, M., Velasco, A. L., Jiminez, F., Marquez, I., Rise, M., 1995. Electrical stimulation of the centromedian thalamic nucleus in control of seizures: Long-term studies. Epilepsia 36, 63–71.

[34] Velasco, M., Velasco, F., Velasco, A. L., Brito, F., Jiminez, F., Marquez, I., Rojas, B., 1997. Electrocortical and behavioural responses produced by acute electrical stimulation of the human centromedian thalamic nucleus. Electroencephalogr. Clin. Neurophysiol. 102, 461–471.

[35] Velasco, M., Velasco, F., Velasco, A. L., Jiménez, F., Brito, F., Márquez, I., 2000. Acute and chronic electrical stimulation of the centromedian thalamic nucleus: modulation of reticulo-cortical systems and predictor factors for generalized seizure control. Archives of Medical Research 31 (3), 304–315.

[36] Vesper, J., Steinhoff, B., Rona, S., Wile, C., Bilic, S., Nikkhah, G., Ostertag, C., 2007. Chronic high-frequency stimulation of the stn/snr for progressive myoclonic epilepsy. Epilepsia 48, 1984–1989.

[37] Voges, J., Volkmann, J., Allert, N., Lehrke, R., Koulousakis, A., Freund, H.-J., Sturm, V., 2002. Bilateral high-frequency stimulation in the subthalamic nucleus for the treatment of parkinson disease: Correlation of therapeutic effect with anatomical electrode position. Journal of Neurosurgery 96, 269–279.